Atmospheric Environment 74 (2013) 326–337

Contents lists available at SciVerse ScienceDirect

Atmospheric Environment

journal homepage: www.elsevier.com/locate/atmosenv

Particle number emission factors for an urban highway tunnel

Jessica L. Perkins [1], Luz T. Padró-Martínez, John L. Durant*

Department of Civil & Environmental Engineering, Tufts University, Medford, MA, USA

HIGHLIGHTS

- Temporal differences in particle number emission factor (EF_{PN}) were measured.
- EF_{PN} was ~2-fold higher in winter and spring compared to summer and fall.
- EF_{PN} was ~2-fold higher in the morning compared to the afternoon/evening.

ARTICLE INFO

Article history:
Received 4 October 2012
Received in revised form
17 February 2013
Accepted 25 March 2013

Keywords:
Traffic-related air pollution
Ultrafine particles
Roadway tunnel
Highway
Temporal variation
Mobile monitoring

ABSTRACT

Exposure to traffic-related air pollution has been linked to increased risks of cardiopulmonary disease, asthma, and reduced lung function. Ultrafine particles (UFP; aerodynamic diameter < 100 nm), one component of traffic exhaust, may contribute to these risks. This paper describes the development of UFP emission factors, an important input parameter for dispersion models used for exposure assessment. Measurements of particle number concentration (PNC), a proxy for UFP, were performed in the Central Artery Tunnel on Interstate-93 in Boston (MA, USA). The tunnel system consists of two, unidirectional bores, which each carry ~9×10^4 vehicles per day (diesel vehicles comprise 2–5% of the fleet in the southbound tunnel and 1–3% in the northbound tunnel). A tunnel was chosen for study because it provided an enclosed environment where the effects of lateral and vertical dispersion by ambient air and photochemical reactions would be minimized. Data were collected using a mobile platform equipped with rapid-response instruments for measuring PNC (4–3000 nm) as well as NO_x. Because Boston is located in a temperate region (latitude 42° N), we were interested in studying seasonal and diurnal differences in emission factors. To characterize seasonal differences, mobile monitoring was performed on 36 days spaced at 7–14 day intervals over one year (Sept. 2010–Sept. 2011); to characterize diurnal differences intensive mobile monitoring ($n = 90$ total trips through the tunnels) was performed over the course of two consecutive days in January 2012. All data collected during congested traffic conditions (~7% of total data set) were removed from the analysis. The median PNC inside the two tunnels for all trips during the 12-month campaign was 3–4-fold higher than on I-93 immediately outside the tunnel and 7–10-fold higher than on I-93 4 km from the tunnel. The median particle number emission factors (EF_{PN}) (±median absolute deviation) for the southbound and northbound tunnels were 5.1×10^{14} (2.3×10^{14}) and 1.4×10^{14} (4.2×10^{13}) particles vehicle^{-1} km^{-1}, respectively. EF_{PN} values were ~2-fold higher in winter and spring (average ambient temperature at the time of monitoring = 6.9 °C) compared to summer and fall (12.9 °C), and ~2-fold higher in the morning (−7.9 °C) compared to the afternoon/evening (−0.9 °C) on two consecutive winter days. Our results suggest that seasonal and diurnal variations in particulate emissions from highway vehicles may be important to consider in developing EF_{PN} values.

1. Introduction

Concern that traffic-generated ultrafine particles (UFP; aerodynamic diameter < 100 nm) may be a risk factor for cardiovascular and respiratory diseases has motivated research to better quantify UFP exposures near busy roadways, where high levels of UFP are typically observed (Brugge et al., 2007; Delfino et al., 2005; Sioutas et al., 2005). Studies have shown that once emitted by vehicles,

* Corresponding author. Department of Civil & Environmental Engineering, Tufts University, 016 Anderson Hall, Medford, MA, USA. Tel.: +1 617 627 5489.
E-mail address: john.durant@tufts.edu (J.L. Durant).
[1] Current address: Dow Chemical Company, Midland, MI, USA.

1352-2310/$ – see front matter © 2013 Elsevier Ltd. All rights reserved.
http://dx.doi.org/10.1016/j.atmosenv.2013.03.046

primary UFP rapidly mix with surrounding air leading to sharp decreases in concentration with distance from roadways (Durant et al., 2010; Karner et al., 2010; Molnar et al., 2002; Pirjola et al., 2006; Zhu et al., 2004). In addition, depending on ambient temperature and the presence of chemical precursors, UFP can undergo reactions (condensation, evaporation, photochemical oxidation) that can cause the number concentration, size distribution and chemical composition to change over relatively short time scales (minutes) and distances (tens of meters) (Morawska et al., 2008; Zhang and Wexler, 2004). In previous work to estimate traffic-generated air pollutant levels near roadways, dispersion models such as CALINE3, CALINE4 and AERMOD have been used. An advantage of dispersion models is that they provide a framework for evaluating the effects of meteorology (wind speed and direction, mixing height) and reactions on air pollutants downwind of sources. Pollutants commonly modeled with line-source dispersion models include carbon monoxide, nitrogen oxides (NO_x), sulfur dioxide, and volatile organic compounds (Benson, 1992; Jerrett et al., 2005; Venkatram et al., 2009; Wilton et al., 2010). In contrast, relatively little work has been done to model dispersion of UFP near roadways in part because UFP emission factors from motor vehicles have not been well characterized.

In this paper we describe our effort to study vehicle exhaust emissions in an urban highway tunnel to estimate particle number emission factors for a mixed vehicle fleet under real-world driving conditions. In fully enclosed tunnels where dispersion and photochemical oxidation of exhaust constituents are reduced relative to ambient air, primary emissions from vehicles can be quantified for different driving conditions. Because pollutant levels tend to increase with distance in unidirectional tunnels, measurements of particle gradients within tunnels coupled with traffic data can be used to estimate emission factors. Emission factors based on actual driving conditions inside tunnels provide a valuable complement to emission factors generated using more standardized approaches (e.g., dynamometer tests), which do not capture the full range of engine types and loads observed for a mixed vehicle fleet operating under real-world conditions (Jamriska and Morawska, 2001).

Our objectives were to characterize UFP levels and emission factors under typical driving conditions in an urban highway tunnel. We studied the Thomas P. O'Neill Jr. Tunnel ("Central Artery Tunnel"), the underground portion of Interstate-93 (I-93) in Boston (Massachusetts, USA; Fig. 1). Air quality data was collected using a mobile monitoring platform. Mobile monitoring is particularly useful for characterizing urban roadways where variations in traffic

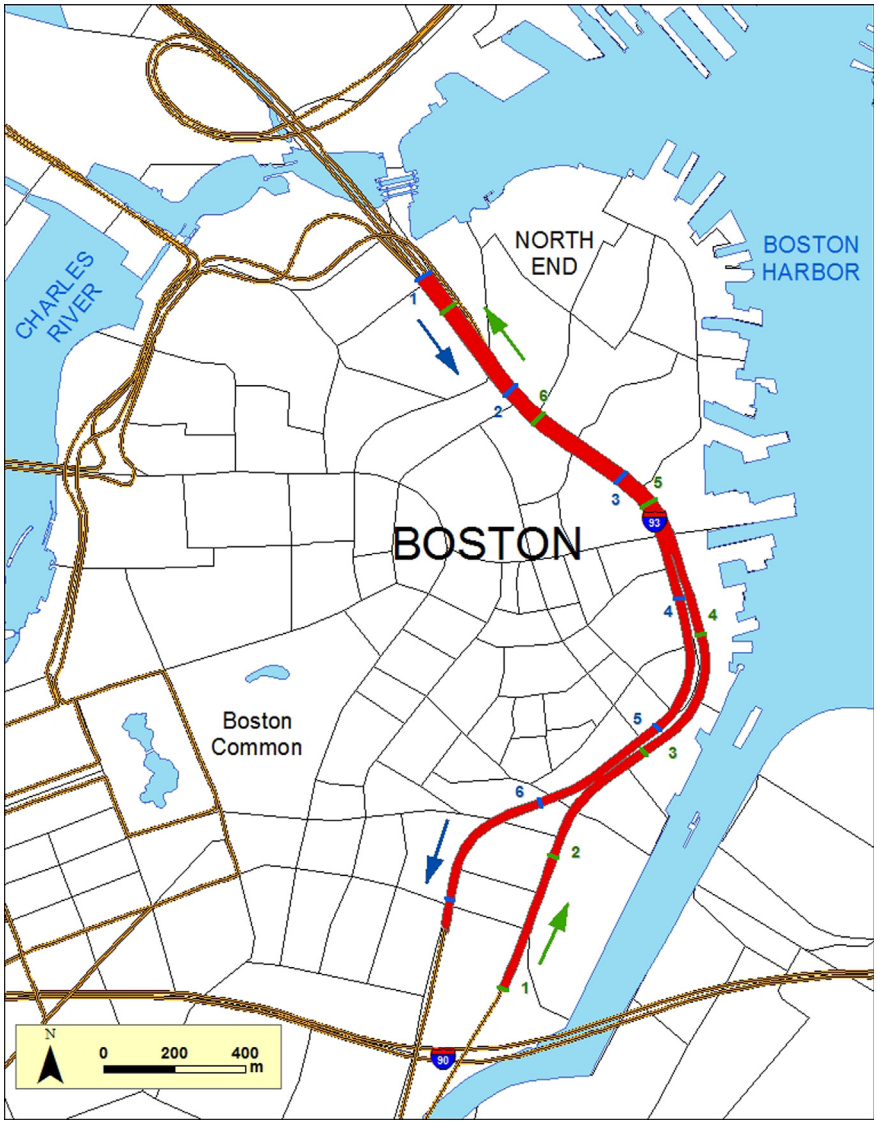

Fig. 1. Central Artery Tunnel in Boston (MA, USA). Arrows indicate traffic direction; numbers and tick marks show the locations of data bins in Fig. 2.

speed and volume, the mix of vehicle types, and traffic entrances and exits can cause small-scale spatial and temporal differences in pollutant levels (Bukowiecki et al., 2002; Weijers et al., 2004; Westerdahl et al., 2005). Previous studies have shown pronounced seasonal and diurnal variations in UFP levels near highways (Charron and Harrison, 2003; Padró-Martínez et al., 2012; Pirjola et al., 2006; Zhu et al., 2004); thus, we were motivated to determine whether these temporal differences in pollutant levels were also reflected in emission rates. Data were collected over the course of one year to capture seasonal differences as well as on two consecutive days of intensive monitoring to characterize diurnal variations. The results of this study could help to inform model development for UFP exposure assessment.

2. Methods

2.1. Tunnel description

The Central Artery Tunnel consists of two unidirectional bores: the southbound bore is 2.46-km long and contains three entrances and four exits; the northbound bore is 2.53-km long and contains two entrances and two exits (Fig. 2). The frontal end of the southbound tunnel and the distal end of the northbound tunnel are coincident with one another, whereas the distal end of the southbound tunnel and frontal end of the northbound tunnel are ~300 m apart (Fig. 1). The tunnels are 5.2 m high and buried 30 m below grade (as measured to the top of the tunnel). The highway slopes downward at a ~3% grade at the frontal ends of the two tunnel bores and ascends with the same slope at the distal end of the northbound tunnel; the highway ascends with a more gradual slope at the distal end of the southbound tunnel. Each tunnel is 3–4 lanes wide and carries 8.8×10^4 vehicles day^{-1} (CTPS, 2012). The I-93 vehicle fleet in Boston is dominated by gasoline-powered vehicles, which make up over 96% of the fleet – as measured at stations #8495 and #8494 near the tunnel entrances (NAVTEQ Traffic, 2012). The posted speed limit in both tunnels is 70 km h^{-1}, except at curves where it is 55 km h^{-1}. The tunnels are mechanically ventilated during emergencies; however, during normal (non-emergency) conditions, which was the case during our study, vehicle exhaust is swept longitudinally by the moving traffic (i.e., the "piston effect") and vented through the distal ends of each tunnel bore and to some degree through entrances and exits along their length (Massachusetts Turnpike Authority, 2006).

2.2. Measurements

On-road monitoring was performed using the Tufts Air Pollution Monitoring Laboratory (TAPL), a mobile monitoring platform equipped with rapid-response instruments (Padró-Martínez et al., 2012). The TAPL was driven at the same speed as tunnel traffic. Separate gas and particle inlets are located on the roof of the TAPL, 3.0 m above the ground and 5.5 m forward of the rear of the vehicle, where engine and generator emissions were exhausted. The particle inlet and manifold were made of stainless steel, and the tubing from the manifold to the particle counter was made of conductive silicone; the gas inlet and the tubing connecting the inlet to the instruments were made of Teflon. The length of all tubing was minimized to reduce loss of particles and gas molecules to the tube walls. Measurements were made of the particle number concentration (PNC; # cm^{-3}) in the 4–3000 nm size range as well as the mixing ratio of nitrogen oxides (NO_x; ppb). We used PNC in the 4–3000 nm size range as a proxy for UFP; based on previous measurements near I-93 in Boston UFP are typically >60–80% of the PNC (Durant et al., 2010; Padró-Martínez et al., 2012). PNC was measured using a TSI Model 3775 condensation particle counter (CPC; reporting frequency 1 s; TSI, Minneapolis, MN). This CPC has a manufacturer-reported upper detection limit of 10^7 particles cm^{-3} and a precision of 10% at $<5 \times 10^4$ particles cm^{-3} and 20% at $<10^7$

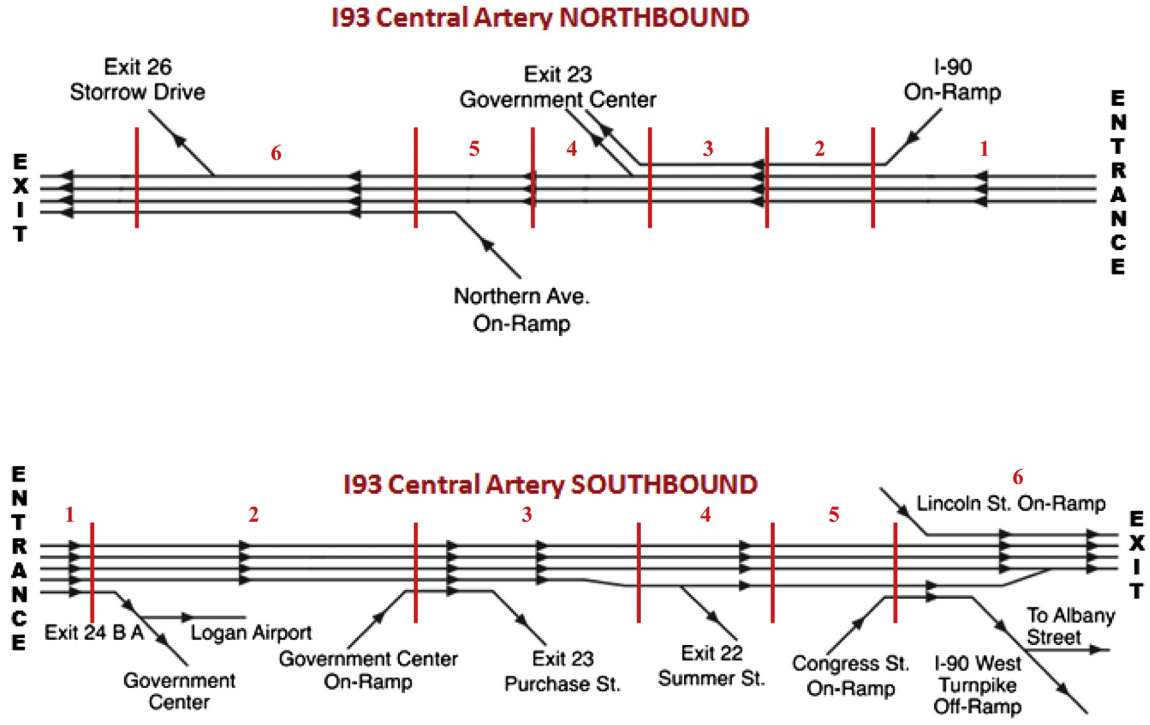

Fig. 2. Schematic of traffic lanes within the northbound and southbound bores of the Central Artery Tunnel including on ramps and off ramps. Data bins, defined by numbers and vertical lines, are measured from the tunnel entrances: (1) 0–400 m, (2) 400–800 m, (3) 800–1200 m, (4) 1200–1600 m, (5) 1600–2000 m, and (6) 2000–2400 m. Schematic is not to scale. Recreated from CTPS (2012).

Table 1
Summary of results from the September 2010 to September 2011 monitoring campaign in the Central Artery Tunnel.

	Southbound tunnel					Northbound tunnel				
Season[a]	Fall	Winter	Spring	Summer	Annual	Fall	Winter	Spring	Summer	Annual
# of trips	9	9	11	4	33	8	9	11	6	34
Total time (min)	21.1	19.1	18.8	8.0	67.0	20.5	19.6	18.7	10.0	68.8
Temperature (standard deviation) (°C)[b]	9.2 (3.6)	0.07 (5.4)	9.7 (7.9)	16.2 (1.9)	8.3 (8.2)	11.2 (4.0)	4.29 (4.6)	11.9 (7.3)	18.4 (4.2)	10.8 (7.0)
Relative humidity (standard deviation) (%)[b]	62.1 (21.5)	53.8 (13.9)	61 (23.9)	68.3 (26.7)	60.5 (20.5)	57 (19.3)	42.3 (17.3)	51.6 (25.7)	63.3 (22.8)	52.8 (21.9)
Median PNC (MAD)[c] (#/cm^3)	2.1×10^5 (5.5×10^4)	5.6×10^5 (1.0×10^5)	4.5×10^5 (2.0×10^5)	2.5×10^5 (4.2×10^4)	4.0×10^5 (1.9×10^5)	2.5×10^5 (1.6×10^5)	6.7×10^5 (2.6×10^5)	2.7×10^5 (1.7×10^5)	2.7×10^5 (2.1×10^5)	2.9×10^5 (1.5×10^5)
Range of PNC (#/cm^3)	5.2×10^4 to 1.4×10^6	9.5×10^4 to 1.9×10^6	4.3×10^4 to 1.3×10^6	2.3×10^4 to 7.1×10^5	2.3×10^4 to 1.9×10^6	7.8×10^3 to 1.0×10^6	3.4×10^4 to 1.8×10^6	2.3×10^4 to 9.7×10^5	3.1×10^4 to 1.5×10^6	7.8×10^3 to 1.8×10^6

[a] Fall = 09/24/10 to 12/21/10; Winter = 12/22/10 to 03/20/11; Spring = 03/21/11 to 06/21/11; Summer = 09/01/10 to 09/23/10 and 06/21/11 to 09/23/11.
[b] Ambient temperature and relative humidity were measured at the MA Department of Environmental Protection air quality monitoring station in Roxbury (#25-025-0042) located ~3 km from the tunnel (MassAir, 2012). The data was averaged for all trips for each season.
[c] Median absolute deviation of PNC.

particles cm^{-3}. All of our measurements were in the 5×10^4 to 10^7 particles cm^{-3} range. A second CPC (TSI Model 3783; size range 7–3000 nm; reporting frequency 1 s) was used to measure PNC inside the cab of the mobile lab during one day of monitoring ($n = 23$ trips through the southbound tunnel). The Model 3783 has an upper detection limit of 10^6 particles cm^{-3} and a precision of 10% at 10^6 particles cm^{-3}. None of the in-cab measurements exceeded 2.6×10^5 particles cm^{-3}. Nitrogen oxides (NO_x; sum of NO_2 and NO concentrations) were measured using a chemiluminescence analyzer (Model 42i, Thermo Scientific; averaging time 10 s). The average travel time in the tunnels was ~120 s, thus 11–12 NO_x and >110 PNC measurements were collected per trip.

The CPCs were manufacturer-calibrated prior to the start of the monitoring campaign. At the end of the study the Model 3775 CPC was compared side by side with an identical, freshly-calibrated unit. Paired measurements differed by <3% and had an R^2 of 0.96. At the start of each monitoring day the CPC flow rates were checked (Defender 510-H, Bios International), and a polyethersulfone membrane filter (rated at 99.96% removal efficiency for 0.45 μm particles) was placed on the inlet to check that the PNC dropped to <100 particles per cm^3. Additional quality assurance measures for data collection with the TAPL have been described elsewhere (Padró-Martínez et al., 2012).

To characterize seasonal differences, monitoring was performed at different times between 05:00 and 20:00 on 36 days (29 weekdays and 7 weekend days) between September 2010 and September 2011. One trip through the southbound tunnel and one through the northbound tunnel were completed on each day of monitoring; the southbound tunnel was monitored first and the northbound tunnel was monitored 3–4 h later. Measurements were made both inside the tunnel and within 400 m of tunnel frontal and distal ends on I-93. In addition, to characterize diurnal differences intensive monitoring was performed on January 4 and 5, 2012; on these two days trips through the tunnel were made at 30 min intervals from 04:00 to 10:30 and 15:00 to 21:30, except during the morning of January 4 when trips were made every 60 min. On January 5 in-cab PNC monitoring was performed in the TAPL as it was driven through the southbound tunnel. The in-cab CPC was positioned ~1 m from the air vents. The heater was on in the TAPL for all trips and the windows were shut. Because the TAPL did not have a recirculation feature, the cabin was continuously refreshed with outside air. Between trips, the TAPL windows were opened for ~1 min to flush the cabin of residual particles.

Tunnel traffic volumes were estimated using actual measured counts and correction factors based on both traffic models and measured counts. Hourly counts for the southbound (counter #8495) and northbound (counter #8494) lanes were obtained from the Highway Division of the Massachusetts Department of Transportation (NAVTEQ Traffic, 2012). These counters were located >500 m from the tunnel entrances. Model estimates of average weekday daily traffic (AWDT) and average weekday hourly traffic (06:00–10:00 and 15:00–19:00) were obtained from the Boston Region Metropolitan Planning Organization (CTPS, 2012). The model predicted traffic volume (veh d^{-1} or veh h^{-1}) after the entrance and exit of each tunnel as well as after each on-ramp and off-ramp within the tunnels. For times when there were no modeled hourly traffic estimates, we used the modeled AWDT (for

Table 2
Results from the January 4 and 5, 2012 monitoring campaign in the Central Artery Tunnel.

Time	04:00–10:30		13:30–22:00	
Tunnel	South	North	South	North
# of trips	20	20	25	25
Total time (min)	47.5	45.2	54.8	55.1
Temperature (standard deviation) (°C)[a]	−7.2 (5.0)	−7.2 (5.0)	−0.9 (3.2)	−0.9 (3.2)
Relative humidity (standard deviation) (%)[a]	43.8 (0.4)	43.8 (0.4)	38.2 (14.9)	38.3 (14.9)
Median PNC in tunnel (MAD)[b] (#/cm^3)	4.1×10^5 (1.1×10^5)	4.0×10^5 (1.2×10^5)	2.9×10^5 (1.0×10^5)	3.3×10^5 (9.9×10^4)
Range of PNC in tunnel (#/cm^3)	2.4×10^4 to 1.6×10^6	1.1×10^4 to 1.5×10^6	3.9×10^4 to 1.5×10^6	2.6×10^4 to 7.9×10^5

[a] Ambient temperature and relative humidity were measured at the MA Department of Environmental Protection air quality monitoring station in Roxbury (#25-025-0042) located ~3 km from the tunnel (MassAir, 2012). The data was averaged for all trips for each time period.
[b] Median absolute deviation of PNC.

hours between 10:00 and 15:00), the 18:00–19:00 hourly estimate (for all times after 19:00), or the 06:00–07:00 hourly estimate (for all times before 06:00). These decision rules, which were applied on 43 of the 162 total monitoring trips in the tunnels, resulted in overestimation of tunnel traffic volume before 06:00 and after 19:00. For weekdays, the following equation was used to estimate tunnel traffic:

$$TV_{estimated,x,t} = TV_{counter,t} \times CF_{counter,t} \times CF_{x,t} \quad (1)$$

In this equation $TV_{estimated,x,t}$ represents the estimated hourly traffic volume at a specific location (x) within the tunnels for each hour of air pollution monitoring (t). $TV_{counter,t}$ represents the measured hourly vehicle counts from the traffic counter for each hour of monitoring. $CF_{counter,t}$ is the correction factor to account for the change in modeled hourly vehicle counts between the traffic counter and the tunnel entrance during each hour of monitoring. This correction factor is needed since there were several highway on and off ramps located between the traffic counters and the tunnel entrances. $CF_{x,t}$ is a correction factor to account for the change in modeled hourly vehicle counts between the tunnel entrance and a specific location within the tunnel for each hour of monitoring. This correction factor was needed because each tunnel contained several side entrances and exits (Fig. 2).

Model estimates of tunnel traffic were not available for Saturdays and Sundays; therefore, for weekend days we used a different equation with correction factors based on highway traffic counts:

$$TV_{estimated,wkend,x,t} = TV_{counter,wkend,t} \times CF_{wkend,t} \times CF_{counter,t} \times CF_{x,t} \quad (2)$$

In this equation $TV_{estimated,wkend,x,t}$ represents the estimated hourly traffic volume on a weekend day at a specific location within the tunnels for each hour of air pollution monitoring. $TV_{counter,wkend,t}$ is the measured hourly vehicle counts from the traffic counters on weekend days for each hour of monitoring. $CF_{wkend,t}$ is the ratio of $TV_{counter,wkend,t}$ to $TV_{counter,Fri,t}$ (the measured hourly vehicle counts from the traffic counters on the Friday prior to the weekend day of interest during the same time (h) the monitoring was done on the weekend day). This correction factor was needed to account for the decrease in traffic counts on the weekends because the traffic models did not report values for the weekend days. $CF_{counter,t}$ and $CF_{x,t}$ are defined identically as in the weekday model above and are based on the weekday model results.

2.3. Data analysis

Monitoring data were aggregated in MySQL (www.mysql.com) using PHP scripts. Data processing consisted of several steps. First, measurements associated with instrument errors, as noted in the daily log, were removed. Next, the timestamps for measurements from each instrument were corrected for the time lag between entry of air into the inlet and the time when concentrations were recorded by the instrument. The lag time for the CPC was measured as the time for combustion emissions introduced at the inlet (e.g., smoke from a lit match) to be detected by the instrument. The lag time for the NO_x instrument, which was slower to respond to sharp increases in pollutant levels, was determined by comparing NO_x peak concentrations in time-series plots to peaks in PNC. In-tunnel peak concentrations of NO_x lagged PNC peaks by on average 41 s. The final step was to remove data that possibly reflected self-sampling of TAPL exhaust. Based on our decision rules for non-tunnel monitoring (Padró-Martínez et al., 2012), we removed data if the TAPL speed in the tunnel was <5 km h^{-1}, which occurred during periods of traffic congestion. All data from 3/36 trips through the south tunnel and 2/36 trips through the north tunnel during the year-long campaign were removed to avoid self-sampling; however, none of the data from the January 4th and 5th 2012 data set was removed. As a result, the emissions factors we report here may contain a possible low bias. Pollutant spikes due to other vehicles, as confirmed by the written daily log, were not removed from the data set. Because the data were not normally distributed, the median and median absolute deviation were used as summary statistics. Statistical analyses were performed using SAS (version 9.2). Plots of pollutant concentration versus distance in the tunnels were created using Igor Pro 6.2.

PN emission factors were estimated using the following method: (1) all PNC measurements collected during a single trip

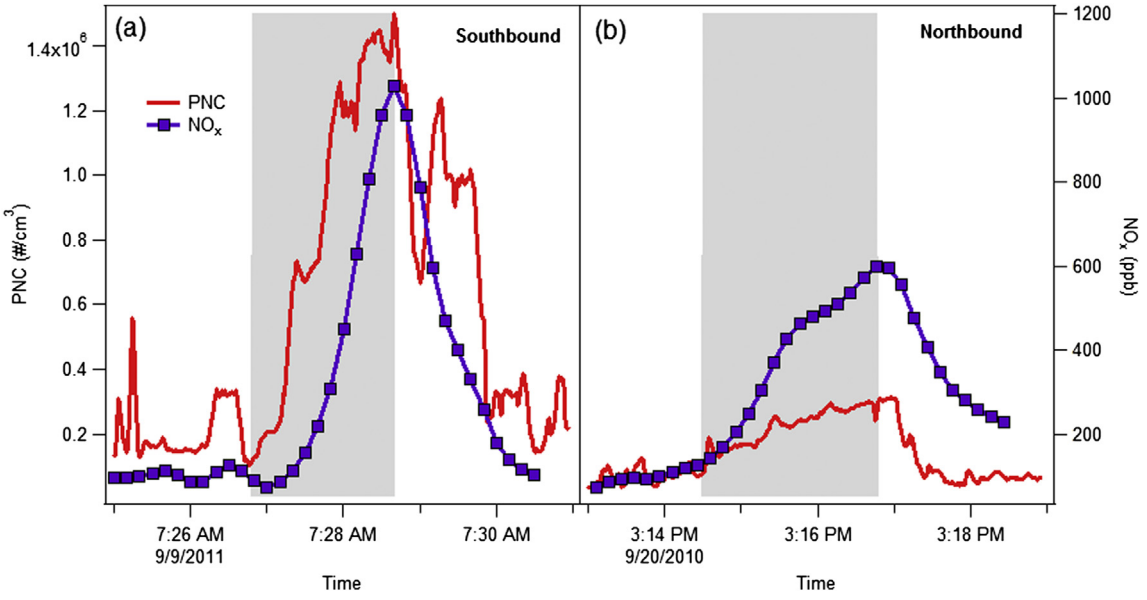

Fig. 3. PNC and NO_x time-series plots for (a) one trip through the southbound tunnel and (b) one trip through the northbound tunnel. The area highlighted in gray indicates when the TAPL was inside the tunnel.

through a tunnel were placed in 400-m bins measured from the tunnel entrance; (2) the median PNC in each bin was then divided by the bin-specific traffic count during the monitoring trip (the estimated average hourly traffic volume determined from equations (1) and (2) was used to generate these values and the results were expressed as # cm^{-3} $vehicle^{-1}$); (3) the estimates from step (2) were then multiplied by the corresponding tunnel air volume to obtain PN per vehicle (# $vehicle^{-1}$); and finally, (4) scatter plots of the PN per vehicle versus distance in the tunnel were created, and the slope of the regression line was taken as the emission factor (EF) in units of # $vehicle^{-1}$ km^{-1}. EFs for NO_x were generated in a similar manner.

3. Results and discussion

The two tunnel bores were monitored once a day on 36 days spaced at relatively even intervals (every 7–14 d) between September 2010 and September 2011 (Table 1). Data from five trips were removed because there was traffic congestion (TAPL speed <5 kmph), which increased the likelihood of self-sampling. In the southbound tunnel one trip was removed in the spring (May 25, 2011) and two in the summer (June 28, 2011 and September 16, 2011); in the northbound tunnel one trip in the spring (May 25, 2011) and one in the fall (September 30, 2010) were removed. After removing these trips, the total time spent monitoring PNC in the southbound and northbound tunnels was 67 and 69 min, respectively. On January 4 and 5, 2012, 45 trips were made in each direction – 22 through each tunnel on January 4 and 23 through each tunnel on January 5. Over these two days, the total time monitoring in the southbound and northbound tunnels was 102 and 100 min, respectively (Table 2). On five trips during the year-long monitoring campaign, the combined effects of NO_x spikes on I-93 outside the tunnel entrances and the slow instrument response time prevented measurement of gradients within the tunnel; thus, NO_x data were removed for these trips.

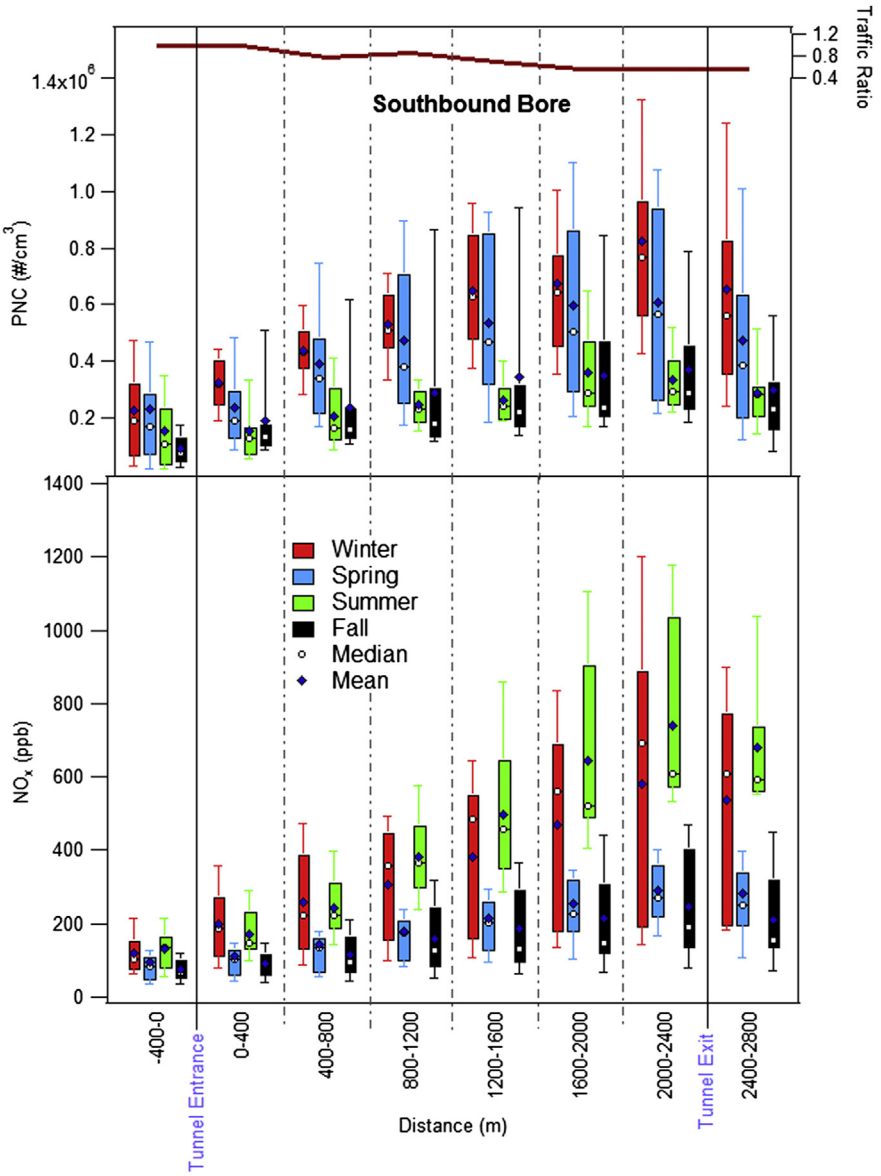

Fig. 4. Seasonal box plots of PNC and NO_x versus distance in the southbound bore of the Central Artery Tunnel during the September 2010–September 2011 monitoring campaign. The whiskers represent the 10th and 90th percentiles. The ratio of the mean traffic volume in each 400-m section to that at the tunnel entrance is shown at the top of the figure. Figures including outliers are presented in Supplementary materials.

3.1. In-tunnel PN and NO_x concentrations

The time-series plots in Fig. 3 show that PN and NO_x levels increased with distance (i.e., time in tunnel) in the two tunnel bores, consistent with expectations for tunnels that were not mechanically ventilated at the time of monitoring. These gradients compare well with Herndon et al. (2005), who used a mobile monitoring platform to measure volatile organic compounds within the southbound bore of the Central Artery Tunnel. The median PN concentrations (±median absolute deviation) in the southbound and northbound tunnels for all trips during the 12-month campaign were 4.0×10^5 ($\pm 1.9 \times 10^5$) and 2.9×10^5 ($\pm 1.5 \times 10^5$) particles cm^{-3}, respectively. These levels were 3- and 4-fold higher than the median PNC <400 m from the south and north tunnel entrances, and 7–10-fold higher than the median PNC measured on I-93 in Somerville, ~4 km north of the tunnel (Padró-Martínez et al., 2012).

The results in Figs. 4 and 5 show that PN concentrations were generally higher during the colder months (winter and spring) than during the warmer months (summer and fall). In the southbound tunnel, the median PNC (±median absolute deviation) for all trips was 5.6×10^5 ($\pm 1.0 \times 10^5$) particles cm^{-3} in the winter and 4.5×10^5 ($\pm 2.0 \times 10^5$) particles cm^{-3} in the spring as compared to 2.5×10^5 ($\pm 4.2 \times 10^4$) particles cm^{-3} in the summer and 2.1×10^5 ($\pm 5.5 \times 10^4$) particles cm^{-3} in the fall. In the northbound tunnel the median PN concentrations in winter and spring were 6.7×10^5 ($\pm 2.6 \times 10^5$) and 2.7×10^5 ($\pm 1.7 \times 10^5$) particles cm^{-3}, and in summer and fall the medians were 2.7×10^5 ($\pm 2.1 \times 10^5$) and 2.5×10^5 ($\pm 1.6 \times 10^5$) particles cm^{-3} (Table 1). These seasonal differences are consistent with previous studies: higher wintertime PN levels were reported in ambient (non-tunnel) air in Rochester, NY (Wang et al., 2011), Helsinki (Hussein et al., 2005; Pirjola et al., 2006), Los Angeles (Zhu et al., 2004), and the Swiss Alps (Weimer et al., 2009). The results of Kittelson et al. (2000, 2004) and Klose

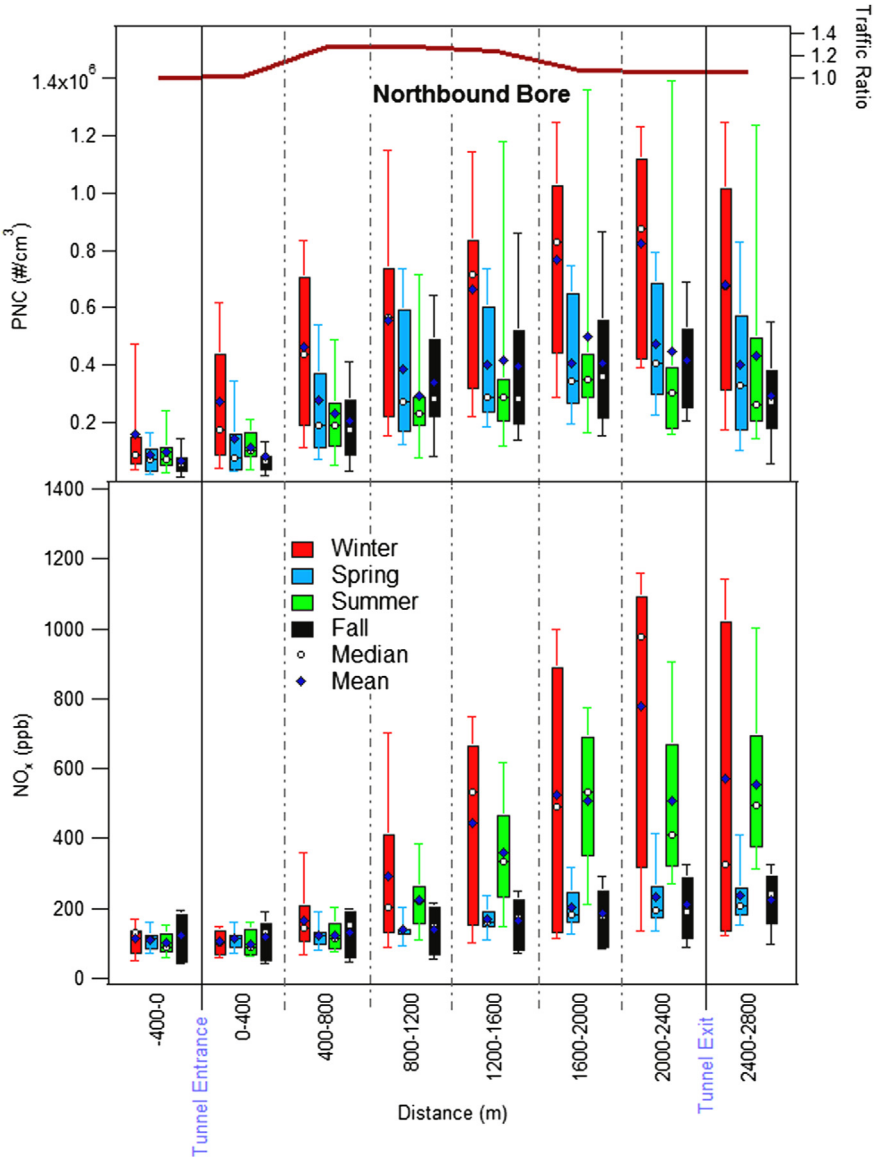

Fig. 5. Seasonal box plots of PNC and NO_x versus distance in the northbound bore of the Central Artery Tunnel during the September 2010–September 2011 monitoring campaign. The whiskers represent the 10th and 90th percentiles. The ratio of the mean traffic volume in each 400-m section to that at the tunnel entrance is shown at the top of the figure. Figures including outliers are presented in Supplementary materials.

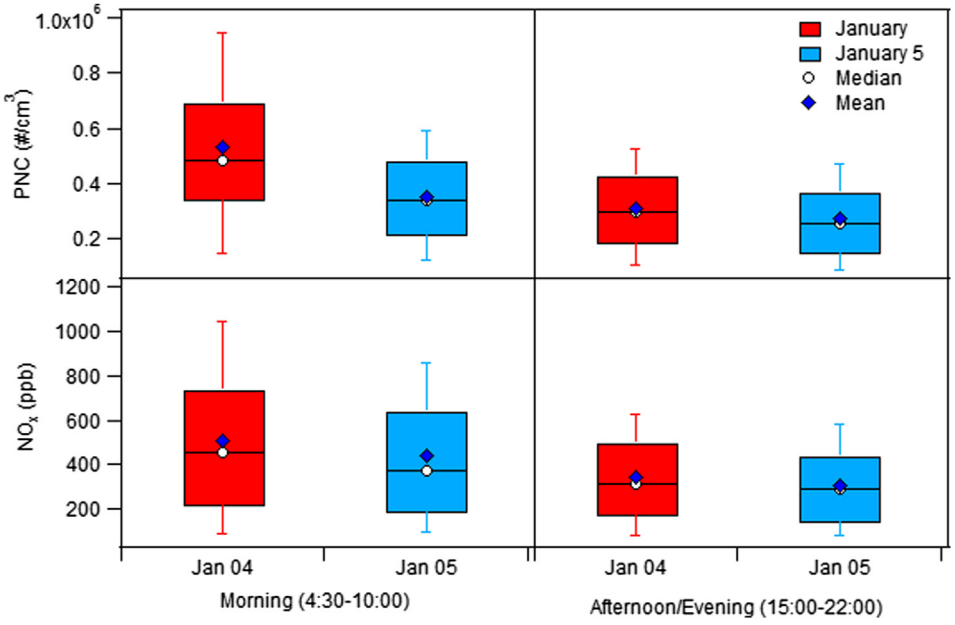

Fig. 6. Diurnal differences in PN and NO_x concentrations based on 90 trips through the southbound and northbound bores of the Central Artery Tunnel on January 4 and 5, 2012. The whiskers represent the 10th and 90th percentiles.

et al. (2009) indicate that higher PN levels in wintertime are attributable to nuclei-mode particles (diameter 5–50 nm), which are formed in greater amounts at colder ambient temperatures, while the formation of accumulation mode and coarse mode particles is largely temperature invariant. The high PNC variability in winter and spring measurements (Figs. 4 and 5) may be attributable to the high temperature variation during winter and spring monitoring (Table 1). As expected, NO_x levels were also elevated in winter (Figs. 4 and 5); however, unlike PN concentrations, which were generally low in summer, NO_x levels were also elevated in summer. This was unexpected; in an earlier study we reported that NO_x levels near I-93 (~4 km north of the tunnel) were lowest in the summer months (Padró-Martínez et al., 2012). Other predictors of NO_x – e.g., diesel vehicles and traffic volumes – were not unusually high during the summertime measurements, and we are thus unable to explain the elevated levels of NO_x in the tunnels during the summer.

The results of monitoring on January 4 and 5 indicate there were diurnal differences in PNC in the tunnel. The overall two-day median PNC from all morning trips (04:00–10:30) through the southbound and northbound tunnels were both ~2-fold higher than the median PNC from all afternoon/evening trips (15:00–21:30) (Table 2; Fig. 6). Like the seasonal differences in PNC, the diurnal differences can also be explained by temperature. The two-day average temperatures during the morning and afternoon/evening trips through the tunnels (both bores) were −7.2 (±5.0) °C and −0.9 (±3.2) °C, respectively. In previous studies by Charron and Harrison (2003), Molnar et al. (2002) and Wehner et al. (2002),

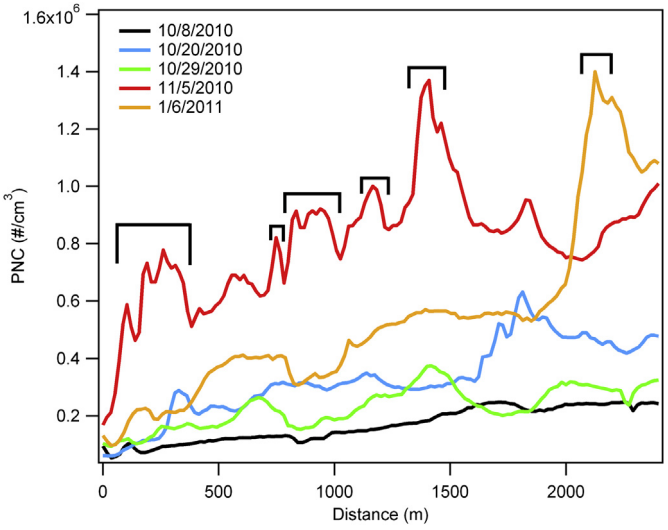

Fig. 7. PNC versus distance for six trips through the southbound tunnel. All trips occurred between 05:15 and 05:30. Heavy-duty diesel vehicles within 3–5 m of the TAPL are indicated by brackets on the November 5, 2010 and January 6, 2011 traces.

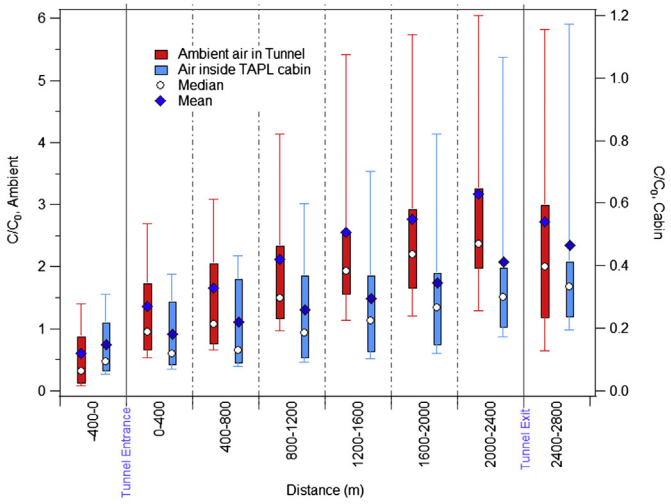

Fig. 8. Box plots of tunnel-air PNC and in-cabin PNC versus distance for 23 trips of the southbound tunnel on January 5, 2012. All measurements were normalized to tunnel entrance air to allow comparison of buildup of PNC in the TAPL cabin relative to ambient levels in the tunnel. The whiskers represent the 10th and 90th percentiles.

Table 3
PN and NO_x emission factors for the southbound and northbound lanes of the Central Artery Tunnel.

Monitoring period	% Diesel vehicles		EF_{PN} (particles veh^{-1} km^{-1})[a,b]		EF_{NOx} (g veh^{-1} km^{-1})[a,b]	
Tunnel	South	North	South	North	South	North
Annual	3.7	2.5	5.1×10^{14} (2.3×10^{14}) $n = 25$	1.4×10^{14} (4.2×10^{13}) $n = 21$	0.369 (0.204) $n = 33$	0.076 (0.039) $n = 24$
Winter	3.4	2.3	7.0×10^{14} (2.0×10^{14}) $n = 7$	1.6×10^{14} (6.7×10^{13}) $n = 7$	0.639 (0.415) $n = 9$	0.318 (0.173) $n = 6$
Spring	4.0	2.4	5.7×10^{14} (2.1×10^{14}) $n = 9$	1.2×10^{14} (4.0×10^{13}) $n = 6$	0.273 (0.074) $n = 11$	0.059 (0.021) $n = 7$
Summer	4.7	3.0	2.1×10^{14} (9×10^{12}) $n = 3$	5.4×10^{13} (2.4×10^{14}) $n = 3$	0.972 (0.129) $n = 4$	0.188 (0.084) $n = 5$
Fall	3.0	2.6	2.7×10^{14} (1.2×10^{14}) $n = 6$	1.4×10^{14} (2.3×10^{13}) $n = 5$	0.203 (0.089) $n = 9$	0.051 (0.013) $n = 6$
January 4 + 5						
04:00–10:00	3.4	2.7	5.5×10^{14} (1.9×10^{14}) $n = 19$	2.0×10^{14} (7.0×10^{13}) $n = 20$	0.992 (0.214) $n = 20$	0.340 (0.121) $n = 20$
15:00–22:00	1.5	1.5	3.3×10^{14} (7.3×10^{13}) $n = 21$	9.2×10^{13} (2.5×10^{13}) $n = 21$	0.729 (0.173) $n = 25$	0.234 (0.062) $n = 22$

[a] Median emission factor with the median absolute deviation shown in parentheses.
[b] Number (n) of trips through the tunnels that yielded data that met all quality assurance requirements.

early morning PNC increases were attributed to higher emissions of particles in the 10–20 nm range. These investigators reported much lower emission of particles in this size range later in the afternoon. Diurnal variations in diesel-vehicle traffic in the tunnel may also help explain our observations. Based on traffic data for January 4 and 5 (2012), diesel vehicles were 2.7–3.4% of the vehicle fleet on I-93 between 04:00 and 10:00 whereas between 15:00 and 22:00 they were only 1.5% of the fleet (NAVTEQ Traffic, 2012). As shown in Fig. 7, PNC spikes in the November 5, 2010 and January 6, 2011 plots are attributable to heavy-duty diesel vehicles (HDDV) within ~3–5 m of the TAPL. During the November 5, 2010 trip the TAPL followed directly behind two diesel trucks after entering the tunnel, and was then passed in succession by a tractor-trailer, a construction vehicle, a school bus, and a panel truck. PNC spikes have also been attributed to HDDVs in several other studies (e.g., Abu-Allaban et al., 2002; Geller et al., 2005; Kirchstetter et al., 2002; Knibbs et al., 2009).

Our results in Fig. 8, which represent 23 trips through the southbound tunnel on January 5, show there was infiltration of particles into the TAPL. In this figure both ambient PNC in the tunnel and PNC inside the TAPL are normalized to ambient PNC at the tunnel entrance to allow comparison of PNC buildup inside the TAPL relative to ambient air in the tunnel. The median in-cab PNC (±median absolute deviation) from all 23 trips was 3.0×10^4 ($\pm 7.6 \times 10^3$) particles cm^{-3}. The infiltration factor – the median of the ratio of the maximum in-cab PNC to the maximum PNC in the tunnel air for all the trips – was 0.30 (note: the maximum in-cab PNC lagged the maximum in-tunnel PNC by about 1 min due to the geometry of the air intake system and fan speed setting). This infiltration factor is consistent with Knibbs et al. (2010) who measured UFP infiltration in vehicles in the M5 East tunnel in Sydney, Australia. Knibbs et al. reported that UFP in-cabin/on-road concentration ratios were as high as ~1.0 when vehicle windows were open, and as low as 0.08 when the vehicle ventilation systems were operating in recirculation mode. Our results may have relevance for in-transit exposure assessment: previous studies have linked exposure to pollutants in tunnel air to increased respiratory health risks (e.g., Larsson et al., 2007; Svartengren et al., 2000).

3.2. Emission factors

The overall median particle number emission factors (EF_{PN}) (±median absolute deviation) – which were based on data from 25 trips through the southbound tunnel and 21 trips through the northbound tunnel on 36 days between September 2010 and September 2011 – were 5.1×10^{14} ($\pm 2.3 \times 10^{14}$) particles

Table 4
PN and NO_x emission factors reported in studies of unidirectional tunnels carrying mixed traffic.

Tunnel/study	Monitoring period[a]	Length (km)	Particle size (nm)	Veh. fleet: % diesel	Veh h^{-1}	Traffic speed (km h^{-1})	PN emission factor[b]	NO_x emission factor[c]
Caldecott, Berkeley, CA; Kirchstetter et al., 2002	July, Aug. 1997 (8 d)	1.1	>10	3.7–4.8	2200	65	2.5×10^{15} (7.5×10^{14})[d]	16.6 (2.0)[d]
				0.29–0.36	4400	59	4.1×10^{13} (6.2×10^{12})[d]	0.799 (0.018)[d]
Caldecott, Berkeley, CA; Geller et al., 2005	Aug., Sept. 2004 (4 d)	1.1	7–270	3.2–4.9	2950	NR	3.2×10^{15} (9.9×10^{14})[d]	NM
				0.25–0.54	4070	NR	2.2×10^{14} (1.2×10^{14})[d]	NM
Tuscarora Mt., Pennsylvania; Abu-Allaban et al., 2002	May 1999 (5 d)	1.6	10–400	>64	200–290	<90	$2.1–3.1 \times 10^{14}$ (NR)	NM
				13–15	550–810	<90	$5.2–5.4 \times 10^{13}$ (NR)	NM
Kingsway Tunnel, Liverpool, UK; Imhof et al., 2006[e]	Feb. 2003 (7 d)	2.48	18–700	7	20,000 d^{-1}	64	1.3×10^{14} (1.0×10^{13})[d]	1.52 (0.3)[f]
Söderledstunnel, Stockholm; Kristensson et al., 2004	Dec. 1998–Feb. 1999	1.5	3–900	5.5	1230	70–90	4.6×10^{14} (1.9×10^{14})[d,g]	1.36 (0.03)[d]
Central Artery Tunnel, Boston; This study	Sept. 2010–Sept. 2011 (31 d)	S: 2.48 N: 2.53	4–3000	2–5	4500	55–70	5.1×10^{14} (2.3×10^{14})[h]	0.369 (0.204)[h]
			4–3000	1–3	5680	55–70	1.4×10^{14} (4.2×10^{13})[h]	0.076 (0.039)[h]

NR = not reported, NM = not measured.
[a] Number of days during which measurements were made are shown parenthetically.
[b] Particles $vehicle^{-1}$ km^{-1}.
[c] grams $vehicle^{-1}$ km^{-1}.
[d] Mean (±standard deviation).
[e] In this study, data collected during periods of lower than normal ventilation rates were excluded from the EF calculations.
[f] Mean (±95% CI).
[g] Adjusted for traffic-speed-dependent particle losses to tunnel walls (at <70 km h^{-1}, only particles >30 nm were considered).
[h] Median (±median absolute deviation).

vehicle^{-1} km^{-1} in the southbound tunnel and 1.4 × 10^{14} (±4.2 × 10^{13}) particles vehicle^{-1} km^{-1} in the northbound tunnel (Table 3). These values are within the range of EFs reported for other unidirectional tunnels carrying mixed fleets of gasoline- and diesel-fueled vehicles (Table 4). EF_{PN} values were generally higher in the southbound tunnel (Fig. 9) due to two factors: (1) compared to the northbound tunnel a greater proportion of monitoring was done in the southbound tunnel during the morning when there were higher numbers of HDDVs on I-93 and lower air temperatures – both of which favor greater PN emissions; and (2) the southbound tunnel carried higher volumes of HDDV compared to the northbound tunnel (3.0–4.7% vs. 2.3–3.0%). Differences in the season-specific EF_{PN} values reflected the seasonal PNC differences (Figs. 4 and 5): median EF_{PN} values were 2.5- and 1.3-fold higher in winter/spring than in summer/fall in the southbound and northbound tunnels, respectively (Table 3; Fig. 9). These seasonal differences do not appear to be driven by differences in diesel traffic, which did not vary significantly with season (Table 3). Similarly, we also observed differences in EF_{PN} values between the morning and afternoon/evening: based on 81 trips on January 4 and 5 (southbound: 19 morning, 21 afternoon; northbound: 20 morning, 21 afternoon), EF_{PN} values were 1.7- and 2.2-fold higher in the morning than in the afternoon/evening in the southbound and northbound tunnels, respectively. Scatter plots and regressions constructed using all of the EF_{PN} and temperature data (Fig. 9c) illustrate the general decrease of EF_{PN} values with temperature. Our results are consistent with those of Klose et al. (2009) who reported that the wintertime EF_{PN} value for Leipzig (Germany) was nearly 2-fold larger than the summertime EF_{PN} value, and that EF_{PN} values were highest during the early morning (00:00–06:00) and relatively constant thereafter.

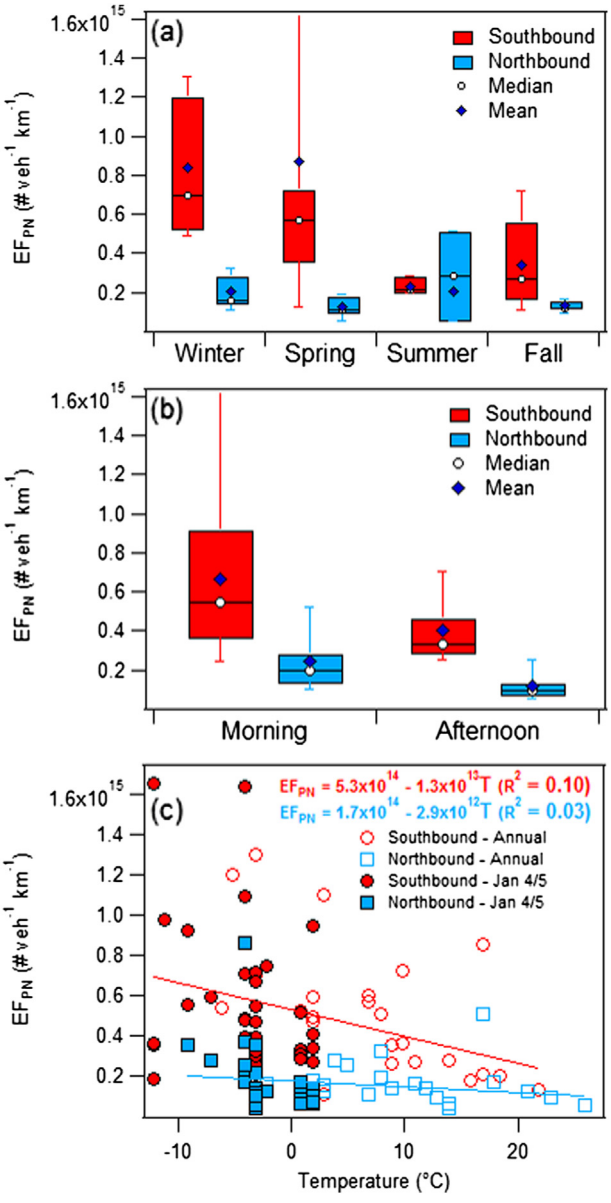

Fig. 9. Box plots of EF_{PN} vs (a) season and (b) time of day based on the data from the year-long campaign. (c) EF_{PN} vs temperature based on data from both the year-long campaign and two days of monitoring in January 2012. The whiskers represent the 10th and 90th percentiles.

The annual median EF_{NOx} values (±median absolute deviation) for the southbound and northbound tunnels were 0.369 (±0.204) and 0.076 (±0.039) g vehicle^{-1} km^{-1}, respectively (Table 3). These values are low compared to estimates reported for other tunnels (Table 4), but are within the ranges reported for specific vehicle types (e.g., AP-42; EPA, 2012). It is possible that our values are lower because we are reporting the medians, whereas the other studies listed in Table 4 reported the means. EF_{NOx} values were highest in the summer followed by winter, spring and fall in that order. The results from two days of intensive monitoring in January (2012) show that EF_{NOx} was ~1.5-times higher in the afternoon/evening compared to the morning (Table 3).

3.3. Significance

The EF_{PN} values we report for the Central Artery Tunnel in Boston are within the range of EFs reported for other unidirectional tunnels carrying mixed fleets of gasoline- and diesel-fueled vehicles (10^{13}–10^{14} particles veh^{-1} km^{-1}) (Table 4). Previous research has shown that fuel type and speed are among the most important factors affecting PN emissions. For example, studies conducted in the Caldecott Tunnel by Kirchstetter et al. (2002) and Geller et al. (2005) and in the Tuscarora Tunnel by Abu-Allaban et al. (2002) show that EF_{PN} values increased with the fraction of diesel vehicles in the fleet by as much as 4–100 fold. Others have shown that EF_{PN} values increased with vehicle speed, particularly for spark-ignition vehicles, due to higher engine loads and exhaust emission rates (Imhof et al., 2006; Jones and Harrison, 2006; Kittelson et al., 2004; Kristensson et al., 2004). Imhof et al. (2006) showed that as vehicle speed increased from 50 to 120 km h^{-1}, EF_{PN} values for spark ignition vehicles increased ~7-fold as compared to only ~1.5-fold for diesel vehicles. Although comparison of PNC measurements between studies is complicated by differences in the size ranges of particles counted (as well as differences in the vehicle fleet composition and traffic speed), the literature generally shows an order of magnitude difference in the range of EF_{PN} for mixed vehicle fleets. Our results complement this literature by showing that seasonal and diurnal differences are important variables to consider when making measurements upon which emission factors will be based. We found that EF_{PN} values were ~2-fold higher in winter and spring (average ambient temperature at the time of monitoring = 6.9 °C) compared to summer and fall (12.9 °C), and ~2-fold higher in the morning (−7.2 °C) compared to the afternoon/evening (−0.9 °C) on two consecutive winter days. While we did not control for vehicle type and speed and engine load, our conclusion that seasonal and diurnal differences are important is supported by studies where seasonal and diurnal variations of PNC in ambient (non-tunnel) air have been observed (e.g., Hussein et al., 2005; Padró-Martínez et al., 2012; Wang et al., 2011; Zhu et al., 2004). Our results may be most relevant for urban areas in

temperate climates where seasonal and diurnal temperature differences are most pronounced.

The motivation of our study was to estimate EF_{PN} values for use in modeling the dispersion of traffic-generated particles near roadways in Boston. In previous studies, dispersion models have been used in combination with field measurements to estimate PN emission factors (inverse modeling). For example, Gramotnev et al. (2003) used measurements from the Gateway Motorway (Brisbane, Australia) and CALINE4 to estimate an average EF_{PN} (2.8×10^{14} particles veh^{-1} km^{-1}) for a mixed-vehicle fleet. Similarly, Birmili et al. (2009) combined PNC measurements made near the A100 motorway in Berlin (Germany) with a 3D dispersion model to estimate an EF_{PN} of 2.1×10^{14} particles veh^{-1} km^{-1}. Also, Zwack et al. (2011) used summertime measurements of PNC in the Williamsburg neighborhood of Brooklyn (NY) – near the Williamsburg Bridge and the Brooklyn-Queens Expressway – along with regression modeling and QUIC (the Quick Urban and Industrial Complex model) to back calculate a EF_{PN} value (5.7×10^{14} particles veh^{-1} km^{-1}). Gidhagen et al. (2003) used wintertime measurements from Söderledstunnel (Stockholm, Sweden) together with a coupled computational fluid dynamics/aerosol dynamics model to estimate EF_{PN} values for different particle sizes and vehicle speeds for both light-duty and heavy-duty vehicles. Based on the results of this study, speed-specific EF_{PN} values for a mixed-vehicle fleet (3.1×10^{14} particles veh^{-1} km^{-1} for <70 km h^{-1} and 4.7×10^{14} particles veh^{-1} km^{-1} for >70 km h^{-1}) were then used in the MATCH model to simulate PNC dispersion in Stockholm (Gidhagen et al., 2005). These studies demonstrate the importance of modeling the major factors that influence PNC variation in urban areas – meteorology, particle dynamics, terrain features and vehicle fleet characteristics. Seen in this light, our findings of modest (~2-fold) differences in EF_{PN} as a function of season and time of day suggest that the need for temperature-specific EF_{PN} values may be less critical than the need for accurate parameterization of other model inputs. On the other hand, there may be value in measuring the temperature dependence of EF_{PN} values in other tunnels, particularly those carrying a higher percentage of diesel vehicles, to determine whether our findings are generalizeable to other areas.

Acknowledgments

We are grateful to Dana Harada, Allison Patton, Piers MacNaughton, Kelsey Perkins, Kevin Stone, Eric Wilburn, Caitlin Collins, and Mariana Liebman-Peláez for helping with data collection and analysis, and to Daniel Chen for producing Fig. 1. Wig Zamore, Doug Brugge, Tom Lisco, George Allen and Mary Davis provided valuable input on study design and data interpretation. This study was funded by the Tufts Institute for the Environment (TIE) and the National Institute of Environmental Health Sciences (Grant No. ES015462).

Appendix A. Supplementary material

Supplementary material associated with this article can be found, in the online version, at http://dx.doi.org/10.1016/j.atmosenv.2013.03.046.

References

Abu-Allaban, M., Coulomb, W., Gertler, A.W., Gillies, J., Pierson, W.R., Rogers, C.F., Sagebiel, J.C., Tarnay, L., 2002. Exhaust particle size distribution measurements at the Tuscarora Mountain tunnel. Aerosol Science & Technology 36, 771–789.

Benson, P.E., 1992. A review of the development and application of the CALINE3 and 4 models. Atmospheric Environment 26B, 379–390.

Birmili, W., Alaviippola, B., Hinneburg, D., Knoth, O., Tuch, T., Borken-Kleefeld, J., Schacht, A., 2009. Dispersion of traffic-related exhaust particles near the Berlin urban motorway – estimation of fleet emission factors. Atmospheric Chemistry and Physics 9, 2355–2374.

Brugge, D., Durant, J.L., Rioux, C., 2007. Near-highway pollutants in motor vehicle exhaust: a review of epidemiologic evidence of cardiac and pulmonary health risks. Environmental Health 6. http://dx.doi.org/10.1186/1476-069X-6-23.

Bukowiecki, N., Dommen, J., Prevot, A.S.H., Richter, R., Weingartner, E., Baltensperger, U., 2002. A mobile pollutant measurement laboratory—measuring gas phase and aerosol ambient concentrations with high spatial and temporal resolution. Atmospheric Environment 36, 5569–5579.

Central Transportation Planning Staff (CTPS) Geoserver, 2012. Traffic Counts on the Central Artery. ftp://ctps.org/pub/Express_Highway_Volumes/20_I93_Central_Artery.pdf (accessed 05.06.12).

Charron, A., Harrison, R.M., 2003. Primary particle formation from vehicle emissions during exhaust dilution in the roadside atmosphere. Atmospheric Environment 37, 4109–4119.

Delfino, R.J., Sioutas, C., Malik, S., 2005. Potential role of ultrafine particles in associations between airborne particle mass and cardiovascular health. Environmental Health Perspectives 113, 934–946.

Durant, J.L., Ash, C.A., Wood, E., Herndon, S., Jayne, J., Knighton, W.B., Trull, J., Brugge, D., Zamore, W., Kolb, C., 2010. Short-term variation in near-highway air pollution gradients on a winter morning. Atmospheric Chemistry and Physics. http://dx.doi.org/10.5194/acp-10-8341-2010.

Environmental Protection Agency (EPA) Modeling and Inventories, 2012. AP-42 Compilation of Air Pollutant Emission Factors. www.epa.gov/oms/ap42.htm (accessed 20.08.12).

Geller, V.D., Sardar, S.B., Phuleria, H., Fine, P.N., Sioutas, C., 2005. Measurements of particle number and mass concentrations and size distributions in a tunnel environment. Environmental Science & Technology 39, 8653–8663.

Gidhagen, L., Johansson, C., Strom, J., Kristensson, A., Swietlicki, E., Pirjola, L., Hansson, H.-C., 2003. Model simulation of ultrafine particles inside a road tunnel. Atmospheric Environment 37, 2023–2036.

Gidhagen, L., Johansson, C., Langner, J., Foltescu, V.L., 2005. Urban scale modeling of particle number concentration in Stockholm. Atmospheric Environment 39, 1711–1725.

Gramotnev, G., Brown, R., Ristovski, Z., Hitchins, J., Morawska, L., 2003. Determination of average emission factors for vehicles on a busy road. Atmospheric Environment 37, 465–474.

Herndon, S.C., Jayne, J.T., Zahniser, M.S., Worsnop, D.R., Knighton, B., Alwine, E., Lamb, B.K., Zavala, M., Nelson, D.D., McManus, J.B., Shorter, J.H., Canagaratna, M.R., Onasch, T.B., Kolb, C.E., 2005. Characterization of urban pollutant emission fluxes and ambient concentration distributions using a mobile laboratory with rapid response instrumentation. Faraday Discussions 130, 327–339.

Hussein, T., Hameri, K., Aalto, P.P., Paatero, P., Kulmala, M., 2005. Modal structure and spatial–temporal variations of urban and suburban aerosols in Helsinki—Finland. Atmospheric Environment 39, 1655–1668.

Imhof, D., Weingartner, E., Prevot, A.S.H., Ordonez, C., Kurtenbach, R., Wiesen, P., Rodler, J., Sturm, P., McCrae, I., Ekstrom, M., Baltensperger, U., 2006. Aerosol and NOx emission factors and submicron particle number size distributions in two road tunnels with different traffic regimes. Atmospheric Chemistry and Physics 6, 2215–2230.

Jamriska, M., Morawska, L., 2001. A model for determination of motor vehicle emission factors from on-road measurements with a focus on submicrometer particles. Science of the Total Environment 264, 241–255.

Jerrett, M., Arain, A., Kanaroglou, P., Beckerman, B., Potoglou, D., Sahsuvaroglu, T., Morrison, J., Giovis, C., 2005. A review and evaluation of intraurban air pollution exposure models. Journal of Exposure Analysis and Environmental Epidemiology 15, 185–204.

Jones, A.M., Harrison, R.M., 2006. Estimation of the emission factors of particle number and mass fractions from traffic at a site where mean vehicle speeds vary over short distances. Atmospheric Environment 40, 7125–7137.

Karner, A.A., Eisinger, D.S., Niemeier, D.A., 2010. Near-roadway air quality: synthesizing the findings from real-world data. Environmental Science & Technology 44, 5334–5344.

Kirchstetter, T.W., Harley, R.A., Kreisberg, N.M., Stolzenburg, M.R., Hering, S.V., 2002. On-road measurement of fine particle and nitrogen oxide emissions from light- and heavy-duty motor vehicles (vol. 33, pg 2955, 1999). Atmospheric Environment 36, 6059.

Kittelson, D., Johnson, J., Watts, W., Wei, Q., Drayton, M., Paulsen, D., Bukowiecki, N., 2000. Diesel aerosol sampling in the atmosphere. SAE Technical Paper 2000-01-2212, http://dx.doi.org/10.4271/2000-01-2212.

Kittelson, D.B., Watts, W.F., Johnson, J.P., 2004. Nanoparticle emissions on Minnesota highways. Atmospheric Environment 38, 9–19.

Klose, S., Birmili, W., Voigtländer, J., Tuch, T., Wehner, B., Wiedensohler, A., Ketzel, M., 2009. Particle number emissions of motor traffic derived from street canyon measurements in a Central European city. Atmospheric Chemistry & Physics Discussions 9, 3763–3809.

Knibbs, L.D., de Dear, R.J., Morawska, L., Mengersen, K.L., 2009. On-road ultrafine particle concentration in the M5 East road tunnel, Sydney, Australia. Atmospheric Environment 43, 3510–3519.

Knibbs, L.D., de Dear, R.J., Morawska, L., 2010. Effect of cabin ventilation rate on ultrafine particle exposure inside automobiles. Environmental Science & Technology 44, 3546–3551.

Kristensson, A., Johansson, C., Westerholm, R., Swietlicki, E., Gidhagen, L., Wideqvist, U., Vesely, V., 2004. Real-world traffic emission factors of gases and particles measured in a road tunnel in Stockholm, Sweden. Atmospheric Environment 38, 657–673.

Larsson, B.-M., Sehistedt, M., Grunewald, J., Skold, C.M., Lundin, A., Blomberg, A., Sandstrom, T., Eklund, A., Svartengren, M., 2007. Road tunnel air pollution induces bronchoalveolar inflammation in healthy subjects. European Respiratory Journal 29, 699–705.

Massachusetts Turnpike Authority, 2006. Central Artery (I-93)/Tunnel (I-90) Project, Operating Certification of the Project Ventilation System. http://www.mass.gov/dep/air/approvals/catsatsd.pdf (accessed 29.02.12).

MassAir, 2012. Station 0042: Boston–Roxbury, MA. MA DEP. http://public.dep.state.ma.us/MassAir/Pages/GetData.aspx?&ht=2&hi=203 (accessed July 2012).

Molnar, P., Janhall, S., Hallquist, M., 2002. Roadside measurements of fine and ultrafine particles at a major road north of Gothenburg. Atmospheric Environment 36, 4115–4123.

Morawska, L., Ristovski, Z., Jayaratne, E.R., Keogh, D.U., Ling, X., 2008. Ambient nano and ultrafine particles from motor vehicle emissions: characteristics, ambient processing and implications on human exposure. Atmospheric Environment 42, 8113–8138.

NAVTEQ Traffic, 2012. http://stakeholder.traffic.com/mainmenu/stakeholder.html (accessed 07.08.12).

Padró-Martínez, L.T., Patton, A.P., Trull, J.B., Zamore, W., Brugge, D., Durant, J.L., 2012. Mobile monitoring of particle number concentration and other traffic-related air pollutants in a near-highway neighborhood over the course of a year. Atmospheric Environment 61, 253–264.

Pirjola, L., Paasonen, P., Pfeiffer, D., Hussein, T., Hameri, K., Koskentalo, T., Virtanen, A., Ronkko, T., Keskinen, J., Pakkanen, T.A., Hillamo, R.E., 2006. Dispersion of particles and trace gases nearby a city highway: mobile laboratory measurements in Finland. Atmospheric Environment 40, 867–879.

Sioutas, C., Delfino, R.J., Singh, M., 2005. Exposure assessment for atmospheric ultrafine particles (UFPs) and implications for epidemiologic research. Environmental Health Perspectives 113, 947–955.

Svartengren, M., Strand, V., Bylin, G., Jarup, L., Pershagen, G., 2000. Short-term exposure to air pollution in a road tunnel enhances the asthmatic response to allergen. European Respiratory Journal 15, 716–724.

Venkatram, A., Isakov, V., Seila, R., Baldauf, R., 2009. Modeling the impacts of traffic emissions on air toxics concentrations near roadways. Atmospheric Environment 43, 3191–3199.

Wang, Y., Hopke, P.K., Chalupa, D.C., Utell, M.J., 2011. Long-term study of urban ultrafine particles and other pollutants. Atmospheric Environment 45, 7672–7680.

Wehner, B., Birmili, W., Gnauk, T., Wiedensohler, A., 2002. Particle number size distributions in a street canyon and their transformation into the urban-air background: measurements and a simple model study. Atmospheric Environment 36, 2215–2223.

Weijers, E.P., Khlystov, A.Y., Kos, G.P.A., Erisman, J.W., 2004. Variability of particulate matter concentrations along roads and motorways determined by a moving measurement unit. Atmospheric Environment 38, 2993–3002.

Weimer, S., Mohr, C., Richter, R., Keller, J., Mohr, M., Prevot, A.S.H., Baltensperger, U., 2009. Mobile measurements of aerosol number and volume size distributions in an Alpine valley: influence of traffic versus wood burning. Atmospheric Environment 43, 624–630.

Westerdahl, D., Fruin, S., Sax, T., Fine, P.M., Siotas, C., 2005. Mobile platform measurements of ultrafine particles and associated pollutant concentrations on freeways and residential streets in Los Angeles. Atmospheric Environment 39, 3597–3610.

Wilton, D., Szpiro, A., Gould, T., Larson, T., 2010. Improving spatial concentration estimates for nitrogen oxides using a hybrid meteorological dispersion/land use regression model in Los Angeles, CA and Seattle, WA. Science of the Total Environment 408, 1120–1130.

Zhang, K.M., Wexler, A.S., 2004. Evolution of particle number distribution near roadways – Part I: analysis of aerosol dynamics and its implications for engine emission measurement. Atmospheric Environment 38, 6643–6653.

Zhu, Y., Hinds, W.C., Shen, S., Sioutas, C., 2004. Seasonal trends of concentration and size distribution of ultrafine particles near major highways in Los Angeles. Aerosol Science & Technology 38, 5–13.

Zwack, L.M., Hanna, S.R., Spengler, J.D., Levy, J.I., 2011. Using advanced dispersion models and mobile monitoring to characterize spatial patterns of ultrafine particles in an urban area. Atmospheric Environment 45, 4822–4829.